

# Surface-Micromachined Microoptical Elements and Systems

RICHARD S. MULLER, LIFE FELLOW, IEEE AND KAM Y. LAU, FELLOW, IEEE

## Invited Paper

*Optical systems are ubiquitous in the present-day societal fabric, from sophisticated fiber-optic telecommunication infrastructure to visual information display, down to mundane chores such as bar-code reading at the supermarket. Most of these existing systems are built from bulk optical components, as they have been for many years. Just as miniaturization and batch-process production have revolutionized electronics, similar advances in optics will certainly greatly expand its applications and markets. Production techniques for optical systems that employ the emerging microelectromechanical systems (MEMS) technologies give promise of achieving this success. Simple micromechanical fabrication techniques are already employed in fiber-optic components to produce what is generally described as silicon-optical-bench systems. New developments, especially those permitting the use of microactuated structures, make substantial increases in system sophistication possible. Surface micromachining, in which microoptical systems are batch-fabricated and placed on top of a silicon wafer, has become a promising approach to this progression. With the demonstration that surface-micromachined elements can be “folded” out from the plane in which they are constructed, an important new degree of design freedom has emerged. This paper examines some of the results obtained and attempts to project possibilities for surface micromachining in future optical systems.*

**Keywords**—Actuated micromirrors, bar-code reader, fiber-optic components, gratings, laser-fiber coupler, optical scanners.

## I. INTRODUCTION

The continuing spectacular growth in optical system applications, as exemplified by optical-fiber telecommunication infrastructure and display technologies, has stimulated great interest in producing miniaturized, reliable, inexpensive photonic devices for light-beam manipulation. There is strong desire for such devices to function without

any mechanical moving parts, out of consideration that these traditionally contribute to high cost and unreliability. For several decades, the only available control options have been those based on electro- or magneto-optic effects. Such devices, however, generally suffer from high costs and typically operate at low efficiencies. In most cases, optical-beam manipulation can be more effectively carried out with movable mechanical elements such as mirrors and shutters, if only these mechanical parts can be built reliably and inexpensively.

Recent developments in the rapidly emerging discipline of microelectromechanical systems (MEMS) show special promise for providing microoptical systems to perform the functions described above. In particular, the technique of *surface micromachining* is interesting in that it is a planar process that is capable of producing large-area, high-quality layered structures along the plane of the substrate, which can then be rotated out of the surface to form large optical surfaces angled to the surface of the substrate. Such large elevated surfaces (up to millimeters in height) with high optical quality, and which are movable with high precision, are very difficult to fabricate with other micromachining technologies.

At the Berkeley Sensor & Actuator Center (BSAC), a background in the development of *surface micromachining* has provided impetus for the development of actuated micromirrors for fiber-optic systems. The basis of our approach in microoptical systems rests on the following developments: methods for making pin joints and moving-element mechanisms [1], comb drives for oscillating systems [2], microvibromotors as actuation elements [3], and folding of surface structures out of the surface plane to form truly three-dimensional structures [4]. Other groups are also active in applying surface micromachining to photonics, demonstrating innovative ways to use this technology [5], [6]. Rather than attempting to capture the full extent of the expanding efforts by all groups working in this field, we focus in this paper on examples drawn from our work at BSAC.

Manuscript received February 25, 1998; revised April 21, 1998. This work was supported in part by a grant from the Hewlett-Packard Science Centers program, in part by the Defense Advanced Research Project Agency, in part by the National Science Foundation, and in part by the Berkeley Sensor & Actuator Center membership.

The authors are with Berkeley Sensor & Actuator Center, Department of Electrical Engineering and Computer Science, University of California, Berkeley, CA 94720-1770 USA.

Publisher Item Identifier S 0018-9219(98)05094-4.

0018-9219/98\$10.00 © 1998 IEEE

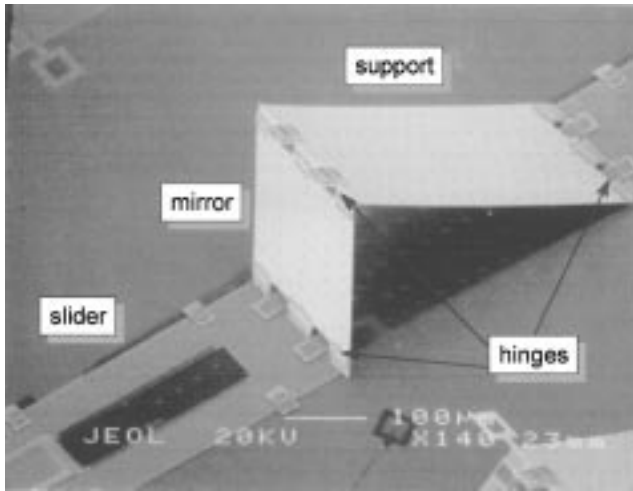


**Fig. 1.** Basic micromirror structure for precision alignment of optical components. The size of the mirror measures approximately  $200 \times 250 \mu\text{m}$ .

## II. OPTICAL MEMS FOR PRECISION ALIGNMENT

### A. Folded-Micromirror Structures

Optical MEMS designed for precision alignment are intended to facilitate automated packaging of optoelectronic devices and subsystems, hence substantially lowering the overall production cost of the modules. Examples of these modules include fiber-pigtailed laser transmitters and external-cavity continuously tunable laser diodes. These modules are expensive because they require submicrometer alignment tolerances that place tight constraints on the positional accuracy of such optoelectronics components as lasers, lenses, gratings, and fibers. Silicon-optical-bench (SOB) technology, commonly used to align optical systems on a silicon substrate using etched v-grooves, solder bumps, and other integrated circuit (IC)-process-derived techniques to achieve  $\pm 1 \mu\text{m}$  transverse alignment [7], [8], is insufficient for high-performance modules. Instead, we promote a paradigm, in which SOB technology—a hands-off automated process—is used for initial placement of the various optical components in the module, followed by an automated active alignment procedure using micromirrors that are prefabricated on the silicon substrate using MEMS technology [9], [10].

Details of a movable micromirror is shown in Fig. 1. It consists of four polysilicon plates, interconnected by three sets of microhinges [11]. The two end plates can slide linearly and independently on the silicon-substrate surface, confined by hubs on the sides. This arrangement provides the mirror with rotational and translational freedom of motion and a high vertical aspect ratio in its operating position.

### B. Vibromotor Actuation

On-chip actuation is necessary in order for the micromachined components to function in a self-contained optical module. There exist numerous ways to achieve on-chip actuation of microstructures; however, actuation of

micromirrors for optical-alignment purposes will need both precision and range—involving mechanisms reminiscent of stepping motors. Here, we describe a specific type of motor that has been successfully employed to drive micromirrors with submicrometer precision and with a range of hundreds of micrometers.

As shown in Fig. 2, each of the two sliders is actuated with an integrated microvibromotor [6], which consists of four electrostatic-comb resonators with attached impact arms driving a slider through oblique impact. (The micromirror shown in Fig. 2 is similar to that shown in Fig. 1 except that the front sliding plate is folded under the back support to save space.) Fig. 3 shows a detailed top view of the vibromotor.

### C. Fabrication

The actuated microreflector was fabricated on a silicon substrate using silicon-surface-micromachining technology. The fabrication process is described in detail in [12]. An  $n^+$  polysilicon layer defines a ground plane. Three additional polysilicon structural layers are used to define the comb drives, sliders, hinges, and mirror beams. Phosphorous-doped silicon dioxide is used for sacrificial spacer layers between polysilicon layers. A special prerelease etch in 5:1 hydrofluoric acid (HF) followed by a vigorous rinse is used to eliminate stringers. Then the structure is released for 10 min in concentrated HF to dissolve the oxide and dried using a critical-point  $\text{CO}_2$  drier [13] to avoid stiction. A  $400 \text{ \AA}$  gold layer is evaporated onto the mirror surface to increase reflectivity.

### D. Actuated Micromirror Characterization

To balance the forces, two opposing impacters are used for each direction of travel. The resonator is a capacitively driven mass anchored to the substrate through a folded-beam flexure. The spring constant of the flexure determines the resonant frequency and travel range of the resonator. The force exerted by the comb drive is proportional to the square of the applied voltage

$$F = \frac{1}{2} \frac{dC}{dx} V^2 \quad (1)$$

where  $V$  typically has both dc and ac components. This quadratic response produces a primary frequency driving term proportional to the product of the dc and ac voltages, effectively linearizing the resonator and increasing the impact force. The comb structures are driven at their resonance frequency (roughly 7.5–8.5 kHz), thereby achieving an amplification of the electrostatic force by the resonator quality factor (typically 30–100 in air [14], [15]). Since energy is transferred to the slider during impact (typically lasting only a few microseconds), the impacters can deliver short-duration forces that are large enough to overcome static friction in the sliders and hinges. Due to the damping (primarily due to air resistance [12]) in the comb structure, the resonators require a few initial cycles to build up sufficient amplitude and momentum for impact. Therefore, in air, slider motion is observed only after three or more

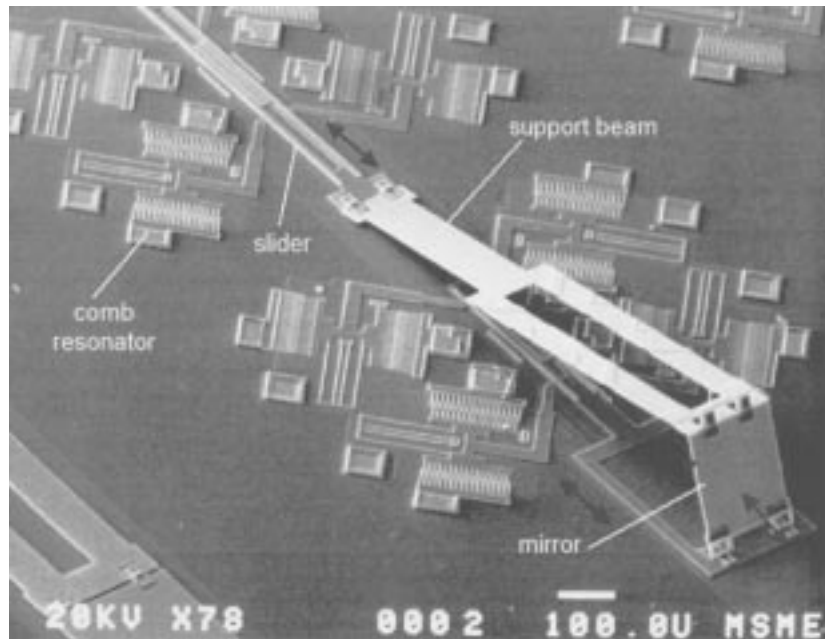


**Fig. 2.** Complete self-actuated micromirror. Two sets of vibromotors, comprising four comb drives each, drive the front and rear sliders for actuation of the mirror.

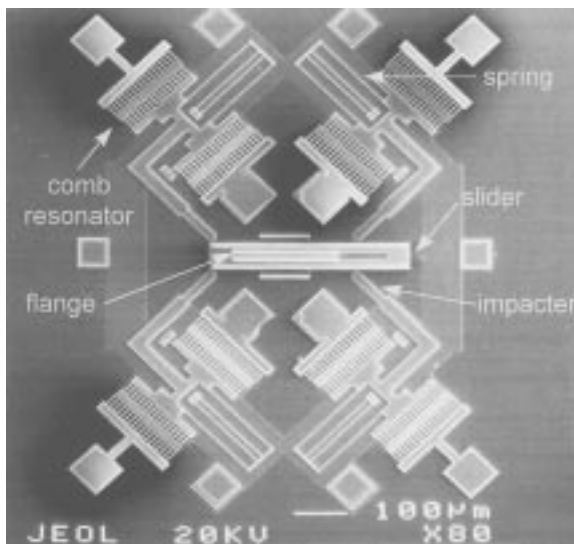


**Fig. 3.** Top view of the linear vibromotor.

voltage cycles. The number of initiation cycles depends on the ambient atmosphere and decreases at lower pressures. When driven with a free-running resonant oscillation, the slider reaches a maximum velocity of over 1 mm/s. Slider velocity can be controlled by driving the comb drives with gated bursts of four to five cycles of the resonant waveform. Once the slider is in position, it is kept in place by static friction until further actuation. Similar structures were previously subjected to shock and vibration tests and showed no detectable slider motion at forces up to 500 G's [12].

Characterization of the vibromotor alone has shown the slider motion to have a step resolution of less than 0.3

$\mu\text{m}$  [12]. To ascertain the performance of the micromirror assembly driven by vibromotors, optical characterization was performed on the integrated microreflector system. A HeNe laser is reflected from the micromirror surface onto a charge-coupled device (CCD) camera. As the front and rear sliders are actuated, the beam position along each of the two axes is measured on the CCD and extrapolated to a location  $200 \mu\text{m}$  in front of the mirror (where a fiber would typically be positioned for a laser-to-fiber coupling application). The standard deviation of the vertical beam position data from a linear response depends on the selected slider step size. For the front slider, this deviation is roughly equal to the step size, while for the rear slider, the deviation exceeds the step size by about 50–60%. The selected average step sizes of  $0.35 \mu\text{m}$  for the front slider and  $0.42 \mu\text{m}$  for the rear slider produce standard deviations of  $0.32$  and  $0.60 \mu\text{m}$ , respectively [Fig. 4(a)]. These deviations are due primarily to the “play” in the hinges and the wobble in the slider structure. The greater length of the rear slider results in increased wobble and leads to a greater standard deviation. The horizontal beam deviation is  $0.05 \mu\text{m}$  [Fig. 4(b)] and is comparable to the  $0.07 \mu\text{m}$  deviation measured in externally actuated structures. This precision is sufficient for laser to single-mode fiber-coupling applications where, due to lens magnification, the beam only needs to be within approximately  $\pm 1 \mu\text{m}$  for high coupling. However, for other advanced optical systems such as tunable external cavity lasers, a higher angular precision is necessary. Since in earlier experiments a microreflector with no on-chip actuators and an alternate hub design has shown a vertical precision of  $0.17 \mu\text{m}$  [12], improving the design of the actuated slider should greatly improve the mirror precision.

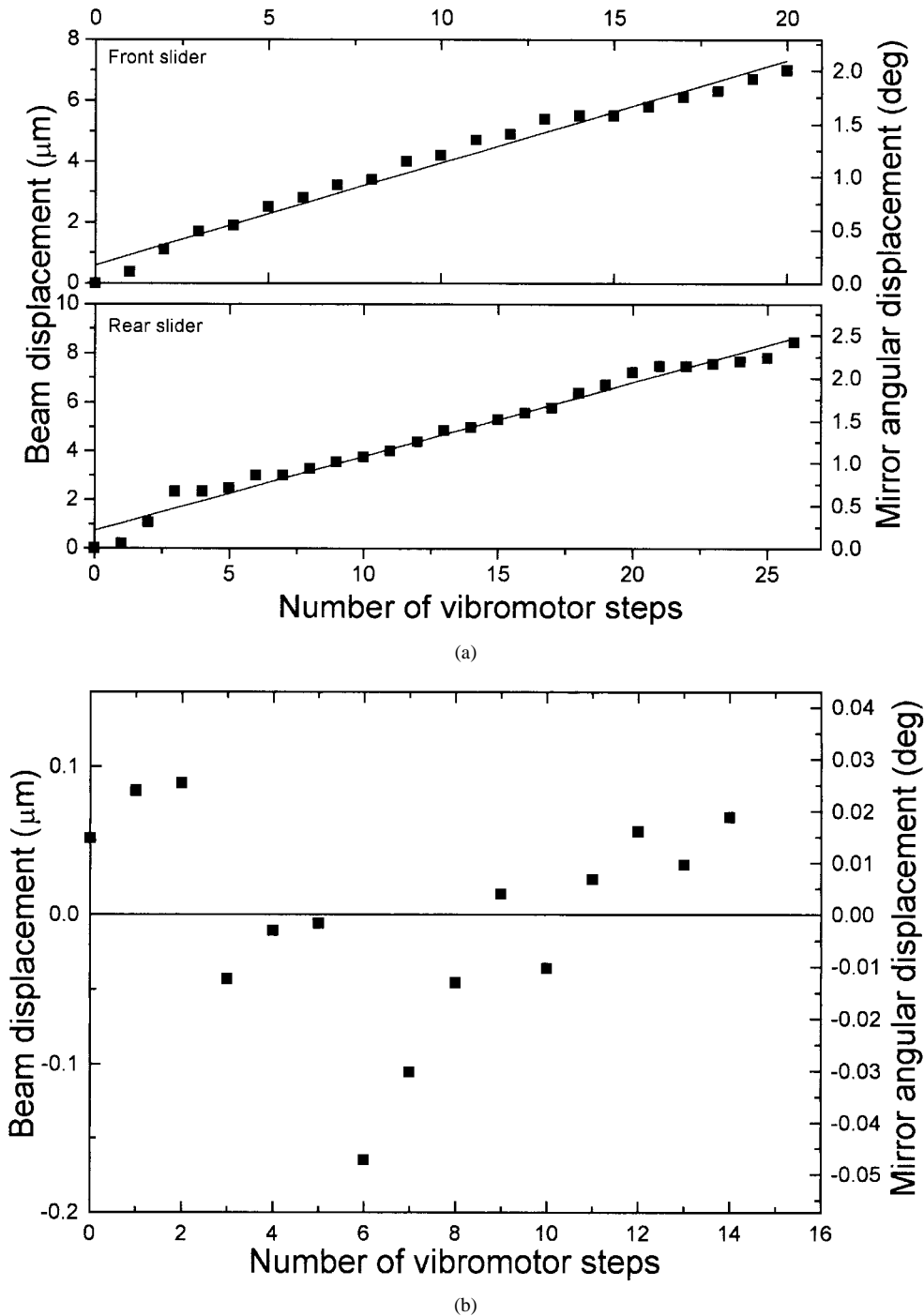


**Fig. 4.** (a) Vertical and (b) horizontal microreflector precision. The vertical position data show standard deviations of  $0.32$  and  $0.6 \mu\text{m}$  (for the front and rear sliders, respectively) from a linear response. The horizontal beam position has an average  $0.05 \mu\text{m}$  of in-plane wobble.

To observe the actuation dynamics of the micromirror, a reflected HeNe beam was imaged on a position-sensitive detector while the angular position of the mirror was swept in real time. The rear vibromotor was biased at  $40 \text{ V}$  dc and driven with  $20 \text{ V}$  (p-p) resonant ( $8.2 \text{ kHz}$ ) square-wave pulses. The position of the beam and the drive voltage were then monitored on a digital oscilloscope. The resulting trace is shown in Fig. 5. As predicted and observed [12], the comb structures require a few cycles (three in this

case) to build up sufficient energy for impact. The first significant impact occurs during the third cycle, at which point the mirror angle begins to change. The mirror is further deflected during the fourth cycle; however, sufficient energy is lost by the resonator to keep the next impact from producing significant displacement. Finally, the sixth cycle provides the greatest impact, resulting in a total mirror rotation of  $0.3^\circ$ . The small back-and-forth motion apparent in the response is most likely due to slight deformation

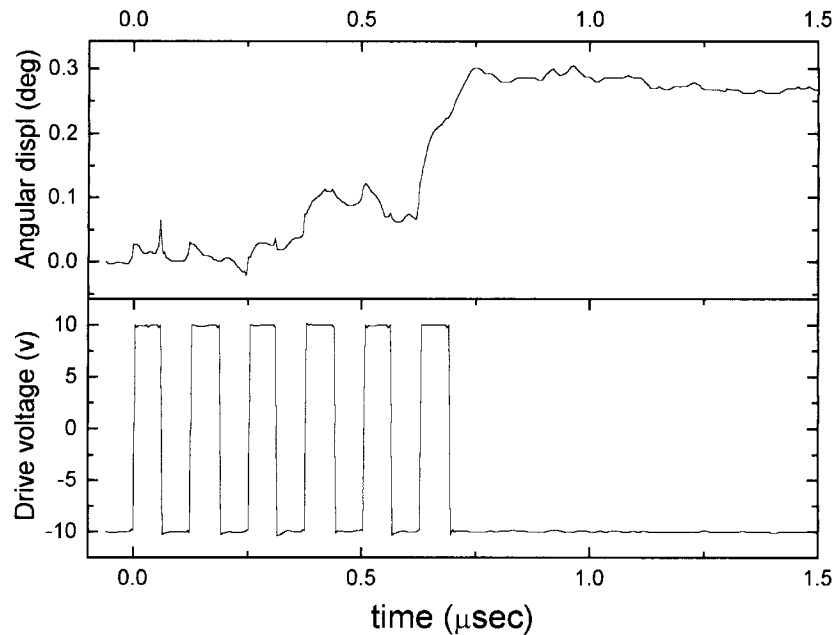


**Fig. 5.** Time-domain response of the microreflector to a square-wave drive voltage. An impact is first achieved during the third cycle, at which point the mirror angle begins to change. The motion concludes shortly after the last cycle, resulting in a total angular displacement of about  $0.3^\circ$ .

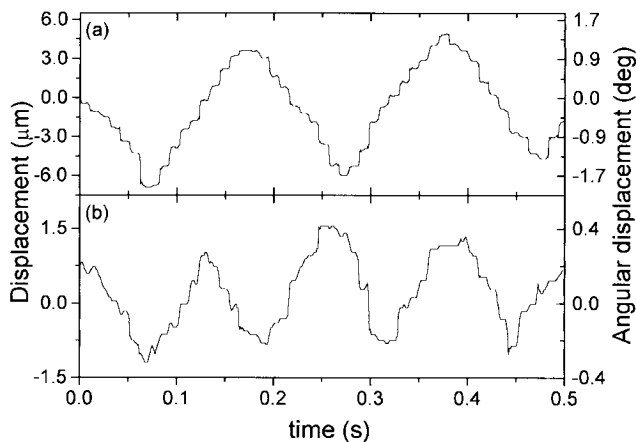


**Fig. 6.** Beam scanning with the actuated microreflector. In (a), a 40-V dc offset was used, resulting in  $0.7\text{--}1.1\ \mu\text{m}$  step size on the plane  $200\ \mu\text{m}$  from the micromirror, while in (b), a 38-V dc offset produces  $0.3\text{--}0.6\ \mu\text{m}$  steps.

of the hinge joints during impact as the square pin is forced against the staple. The remaining “roughness” of the response is due to noise in the detector.

To demonstrate the use of the actuated microreflector in scanning and beam-positioning applications, the mirror was used to scan a laser beam across the detector continuously. The rear vibromotor was driven with bursts of four 20 V (p-p) resonant (8.2 kHz) square-wave cycles spaced 10 ms apart, with a 40- or 38-V dc offset. The resulting output (Fig. 6) clearly shows the step-wise nature of the mirror motion. The average speed of the sweep can be changed by varying the spacing of the bursts. Fig. 6(a) and (b) also demonstrates that the size of the step itself depends on the applied voltage and can be controlled. With an average angular step size of 5 mrad, the microreflector has a

maximum estimated scan rate of 10.2 rad/s or a beam speed of 2 mm/s on a plane  $200\ \mu\text{m}$  in front of the reflector.

#### E. A Single-Mode-Fiber Laser Transmitter Module

The actuated microreflector system is used in a laser-to-fiber coupling module, as illustrated schematically in Fig. 7(a). A picture of the assembled coupling module is shown in Fig. 7(b). An aspheric microlens was used to image the output of a laser diode into a single-mode fiber. A polysilicon micromirror with two degrees of freedom (linear displacement and angular position) reflects the laser beam at a  $45^\circ$  angle and provides the fine alignment. Lens, laser, and fiber are positioned passively on the substrate using etched alignment grooves and photolithographically defined alignment aids and held in place by low-viscosity epoxy. The height of the fiber core is controlled by mounting it in a silicon subcarrier that is attached to the foundation substrate. Using these techniques, the axial displacement and tilt of the optical components can be minimized, and the reduction in coupling efficiency resulting from these sources of misalignment is negligible. Transverse misalignment of the laser and lens, however, has a significant effect on the coupling, particularly because of the magnification of the lens system. As a consequence of our simple passive-alignment method, the transverse offsets of the laser and lens are on the order of  $5\text{--}10\ \mu\text{m}$ , which, magnified by the lens, lead to roughly a  $20\text{--}40\ \mu\text{m}$  displacement of the beam on the fiber plane. Therefore, the micromirror must have sufficient travel range to compensate for these offsets.

This coupling module is used to couple light from a standard telecommunications-grade  $1.3\ \mu\text{m}$  distributed feedback laser into a  $9\ \mu\text{m}$  core single-mode fiber. The actuated microreflector was positioned between the lens and the fiber

# Explore Litigation Insights

Docket Alarm provides insights to develop a more informed litigation strategy and the peace of mind of knowing you're on top of things.

## Real-Time Litigation Alerts



Keep your litigation team up-to-date with **real-time alerts** and advanced team management tools built for the enterprise, all while greatly reducing PACER spend.

Our comprehensive service means we can handle Federal, State, and Administrative courts across the country.

## Advanced Docket Research



With over 230 million records, Docket Alarm's cloud-native docket research platform finds what other services can't. Coverage includes Federal, State, plus PTAB, TTAB, ITC and NLRB decisions, all in one place.

Identify arguments that have been successful in the past with full text, pinpoint searching. Link to case law cited within any court document via Fastcase.

## Analytics At Your Fingertips



Learn what happened the last time a particular judge, opposing counsel or company faced cases similar to yours.

Advanced out-of-the-box PTAB and TTAB analytics are always at your fingertips.

## API

Docket Alarm offers a powerful API (application programming interface) to developers that want to integrate case filings into their apps.

## LAW FIRMS

Build custom dashboards for your attorneys and clients with live data direct from the court.

Automate many repetitive legal tasks like conflict checks, document management, and marketing.

## FINANCIAL INSTITUTIONS

Litigation and bankruptcy checks for companies and debtors.

## E-DISCOVERY AND LEGAL VENDORS

Sync your system to PACER to automate legal marketing.